

NSC-174

# Daytime Whistler-Mode Attenuation through the Lower Ionosphere at 15.5 Kc as Measured on Explorer VI during Launch Trajectory<sup>1</sup>

BY R. F. MLODNOSKY<sup>2</sup>

*Radioscience Laboratory  
Stanford University*

BY R. A. HELLIWELL AND L. H. ROEDEN

*Stanford Research Institute*

Signals from the U.S. Navy Station NSS (15.5 kc) were detected over the altitude range of zero to about 160 km by a satellite-borne VLF receiver during the daytime launch phase of the Explorer VI Satellite. The signals were received on a small electric antenna which was also used simultaneously to transmit VHF telemetry. During the launch phase, the antenna was confined between the third-stage rocket case and the folded solar paddles, with an epoxy shroud covering the satellite and the third-stage rocket. Nevertheless, signals were clearly visible in amplitude-time chart recordings (50-cps bandwidth) up to 67 km altitude. The signal variations between 67 km and 160 km were obtained by narrow-band cross-correlating filter techniques. The receiver output was interpreted in terms of incident electric field strength, and the total measured attenuation through the lower ionosphere up to 160 km was estimated to be 43 db. A predicted total attenuation was computed including the effects of absorption, the change in antenna impedance within the ionosphere, reflection losses and antenna polarization. The predicted and measured attenuations are in good agreement. The measurements are compared with those of relevant rocket and satellite experiments. It is concluded that the launching of the whistler mode, at least in daytime, can be described by utilizing a sharply-bounded model of the ionosphere to account for the reflection-transmission phenomenon, and a slowly-varying model to account for the absorption experienced by the transmitted wave.

## INTRODUCTION

The Explorer VI Satellite was launched from Cape Canaveral at about 0930 Eastern Standard time on 7 August 1959. Among the scientific instruments aboard this satellite was a calibrated VLF receiver designed to study whistler-mode propagation and ionospheric noise.<sup>1,2</sup>

<sup>1</sup> This manuscript was submitted for publication, but the untimely death of the principal author has prevented final revision.

<sup>2</sup> Deceased June 24, 1963.

<sup>3</sup> Superior numbers in text designate References.

The receiver was designed to receive transmissions from the U.S. Navy Station NSS (15.5 kc) at Annapolis, and had a dynamic range of about 80 db and a 3-db bandwidth of 100 cps.<sup>3</sup>

Signals were to be received on a small electric antenna which was used simultaneously to transmit VHF Telemetry. The antenna consisted of two linear elements, about three-fourths of a meter long, approximately parallel to the satellite spin axis (and the rocket longitudinal axis before rocket-satellite separation). The

FACILITY FORM 502

N 66-80540

(PAGES)

CR-68496  
(NASA CR OR TMX OR AD NUMBER)

(THRU)

(CODE)

(CATEGORY)

elements were electrically connected and functioned at VHF as a monopole relative to the satellite body. The undetected receiver intermediate-frequency output was telemetered in analog form beginning before lift-off and continuing throughout the launch until the rocket went over the horizon from Cape Canaveral. The data were obtained during undisturbed ionospheric conditions and thus afforded the opportunity to study the propagation of VLF radio waves through the lowest layers of the "quiet" ionosphere.

In order to interpret the data, it is essential to have a clear understanding of the satellite environment during the launch period. The satellite proper was mounted so that the forward end of the third-stage rocket was located between the antenna elements. The solar paddles were folded over the antenna, reducing the sensitivity by an estimated 30 db. (This sensitivity change was estimated by comparing measurements made on a model of the satellite with paddles erected, with measurements made on the actual satellite mounted on a floor-stand pedestal with paddles folded.) In addition, an epoxy shroud covered the entire satellite and third-stage rocket. The above conditions apply to all data that will be utilized here. The small amount of data obtained after the epoxy shroud was jettisoned could not be meaningfully interpreted.

An initial examination of chart recordings of the data in a 50-cps bandwidth revealed that, in spite of the above shielding of the antenna, NSS signals were detected up to an altitude of about 67 km. The signal disappeared into the noise background at the most interesting altitudes; namely just as the vehicle entered the D-region. The data were extended in altitude with the aid of cross-correlating, narrow-band filtering techniques.

The receiver output variations were referred to the receiver input and interpreted in terms of incident relative electric field strength. Calculations of whistler-mode absorption were made for various electron density and collision frequency models of the lower ionosphere. Absorption and other attenuating effects were combined to estimate a predicted total attenuation. The predicted attenuation was found

to be in good agreement with the measured value.

## DATA ANALYSIS

The undetected output of the VLF receiver was heterodyned down to 2.932 kc in the satellite and added to the telemetry baseband. At the ground station, VLF receivers also monitored station NSS. The NSS signal received on the ground was heterodyned down to 0.884 kc and recorded without rectification together with the telemetry baseband. Thus, the magnetic tape data recordings contained both the output of the satellite VLF receiver and the output of the ground VLF receiver.

The satellite and ground receiver outputs were selected (by filtering—50 cps bandwidth), then rectified and presented in amplitude-time chart recordings. An important section of the launch chart-recording is shown in figure 1. The top channel is the rectified ground receiver output, and shows a normal sequence of dots and dashes in the Morse code. The bottom channel is the rectified satellite receiver output. Timing marks are shown on the upper event-marker channel. Amplitude calibration pulses appear about every 30 seconds in the satellite channel. A good quality calibration pulse is shown between the sections labeled loop 19 and loop 24. Each calibration pulse consists of two levels, the first of which calibrates the receiver and the second of which measures the magnitude of the antenna impedance.

In the satellite channel, the NSS signal amplitude decreases quickly, disappearing into the increasing noise background at about 67 km (within the portion labeled loop 11). The increasing telemetry noise level at just above this altitude is believed to be associated with the interaction of the vehicle and the ionosphere and its discussion is outside the scope of this paper. Before the signal disappeared into the noise, as shown in figure 1, its amplitude was determined by comparison with the calibration pulse amplitudes. The amplitude variations of receiver output below 67 km were scaled directly from the chart recordings and are given in figure 2. Sufficient points are plotted to represent the detailed variations exhibited by the data.

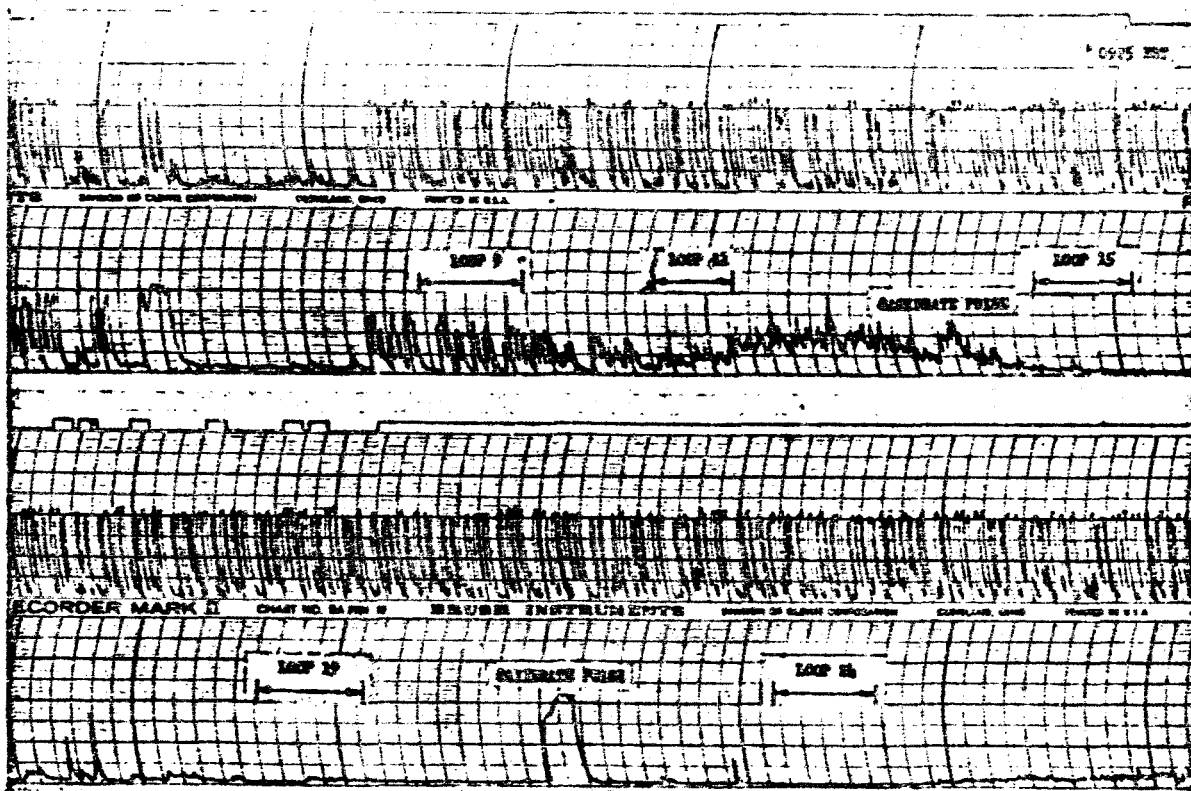


FIGURE 1.—Section of chart recording of the launch data. Upper channel is detected ground receiver output. Bottom channel is detected satellite receiver output.

The receiver output variations after the signal disappeared into the noise were measured with the aid of cross-correlating, narrow-band filtering techniques. A block diagram of the device used is shown in figure 3. The basic principle is bandwidth reduction, achieved by the heterodyning of the satellite receiver output  $f_s$  to a center frequency of 100 cps where narrow bandwidths are easily realized. Post-detection filtering was also employed. Referring to figure 3, it can be seen that the satellite receiver output is heterodyned in Mixer No. 3. The portion of the satellite receiver output spectrum to be examined was selected by adjustment of the mixing frequency ( $3kf_s - f_s$ ). The fixed component of the mixing frequency  $3kf_s$  was generated by the frequency multiplying circuitry from either an audio oscillator  $f_a$ , or the ground receiver output  $f_g$ . The variable frequency component  $f_s$  was generated by a voltage controlled oscillator (VCO). Provi-

sions were made for the manual adjustment or periodic control of the VCO with a function generator. The filtering operations indicated in the block diagram were performed by switch-selected components to provide for faster-than-real-time data processing.

When the audio oscillator was used, the mixing frequency signal was continuous and the device operated solely as a narrow-band filter. When the ground receiver output was used, the mixing frequency signal was present only when NSS was keyed on. This mode of operation is equivalent to cross-correlation between the satellite signal and the essentially noiseless ground-channel information. Cross-correlation in this case reduces the average noise power relative to the average signal power. No provisions were made for adjusting the time delay, and thus the cross-correlation mode was useful only when the delay between the satellite and ground receiver signals was negli-

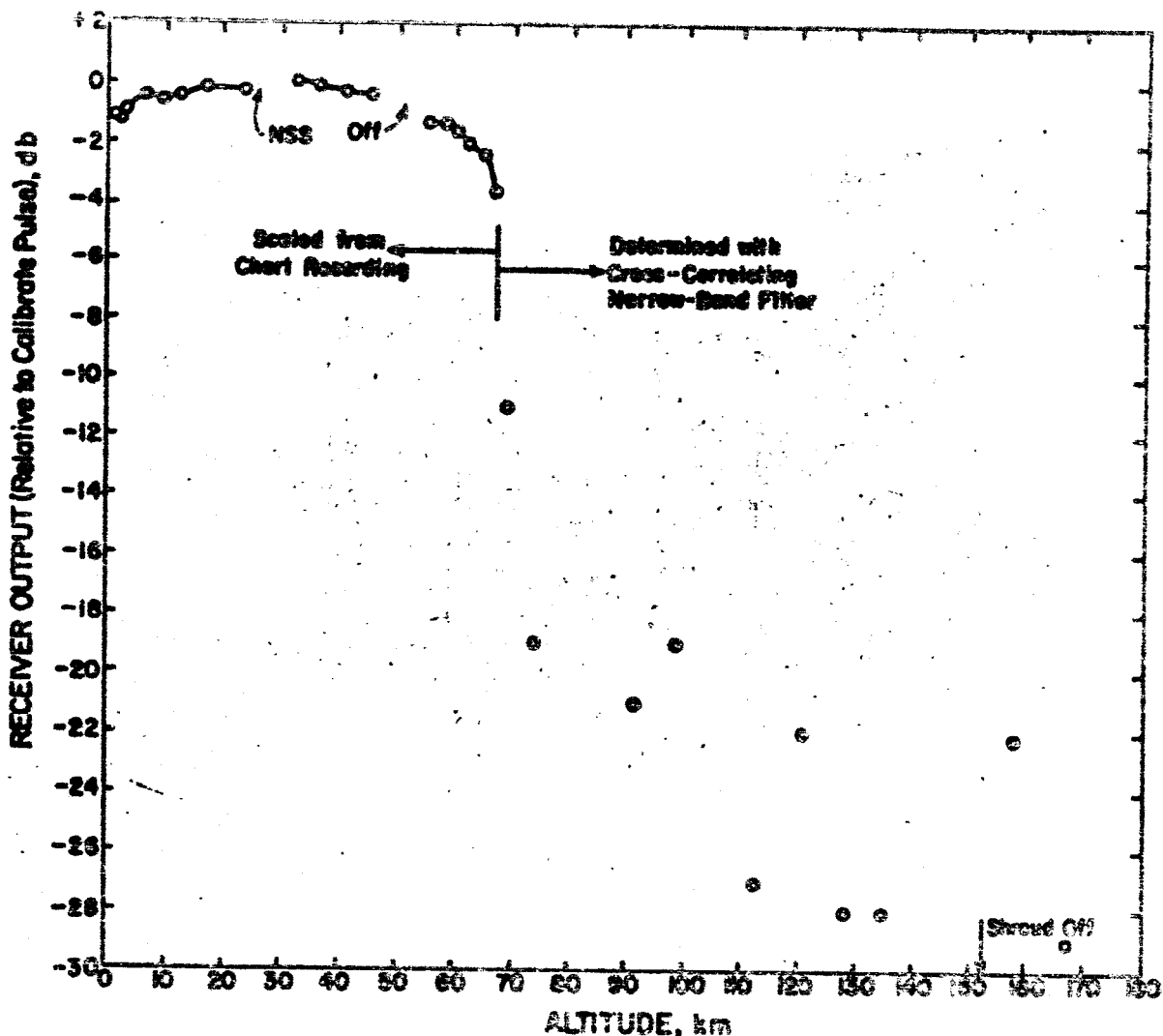


FIGURE 2.—Satellite receiver output level relative to calibrate pulse plotted vs. altitude.

gible with respect to the time scale of NSS traffic. During launch the time delay was assumed to be negligible.

The device described above was used with the launch data in the cross-correlation mode at twice normal tape-playback speed. A predetection bandwidth of 1.7 cps and a 12.0-second post-detection time constant were used. The ground receiver output supplied the fixed frequency component of the mixing frequency. It was found that with the above equipment adjustments, maximum spectral detail was obtained and the measurements were repeatable. Smaller predetection bandwidths were

not useful because of tape recorder limitations. Sections of records to be analyzed were re-recorded on magnetic tape loops which contained 4 seconds of real-time data. While a tape loop was circulating, the VCO was manually advanced and the loop allowed to circulate until a steady output was achieved. The result was a spectrum for each 4-second section of the receiver output data.

Selected examples of the spectra obtained are shown in figure 4. The corresponding sections of the chart recording are labeled with the appropriate tape-loop numbers in figure 1. Although 25 loops were made,

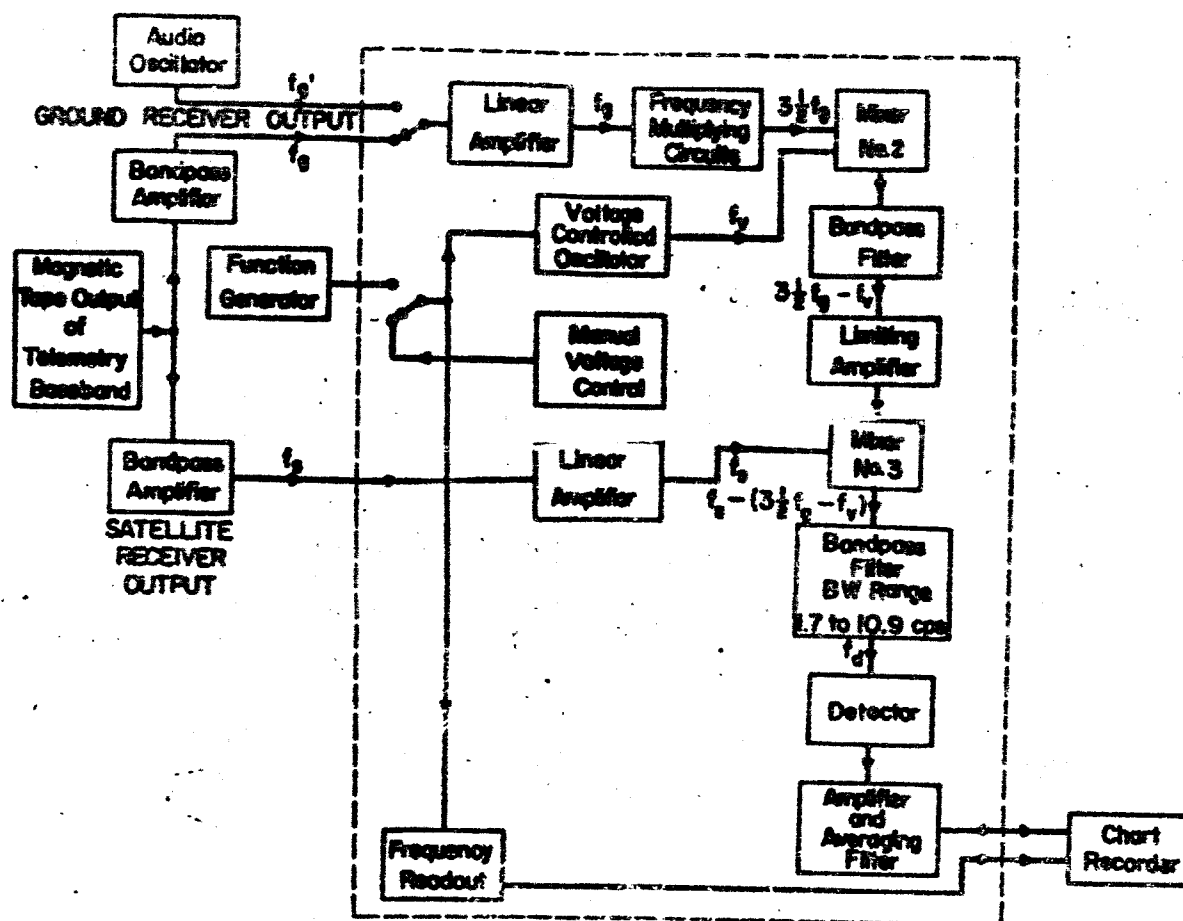


FIGURE 3.—Block diagram of cross-correlating narrow-band filter.

certain loops were discarded because they contained impulsive noise or calibration pulses. It should be noted that the frequency scale in figure 4 is slightly nonlinear. No absolute frequency scale is given because of slow (order of hours) frequency drifts in the system. The limits of the 50 cps noise bandwidth were relied upon for approximate frequency identification within any given spectrum.

The spectrum of loop 9 is in a portion of the data where the NSS signal is readily visible in the chart-recording, and the spectrum of NSS traffic is clearly defined. The succeeding loops exhibit less signal as can be seen in figure 4, and the spectra are more complex. Loop 13 shows small secondary peaks on either side of the central spectrum. This phenomenon is enhanced in loop 19. The exact cause of these secondary peaks is not known, but may be some form of

interference. The appearance of these spectra suggests some form of amplitude modulation of the NSS signal as received at the satellite, although the mechanism for such modulation is not obvious. It was assumed, a priori, that the level of NSS signal is measured by the central peaks in these spectra. The most convincing support for this assumption lies in the systematic and meaningful variation of the electric field strength with altitude which is ultimately defined. The probability that various random noise or interference sources could produce the systematic variation obtained must be exceedingly small.

The relative level of the signals in the spectra was determined by comparing the central peaks in the spectra to the peak in a reference spectrum where the signal was scaleable on the chart recording (loop 9 in this case) and then account-

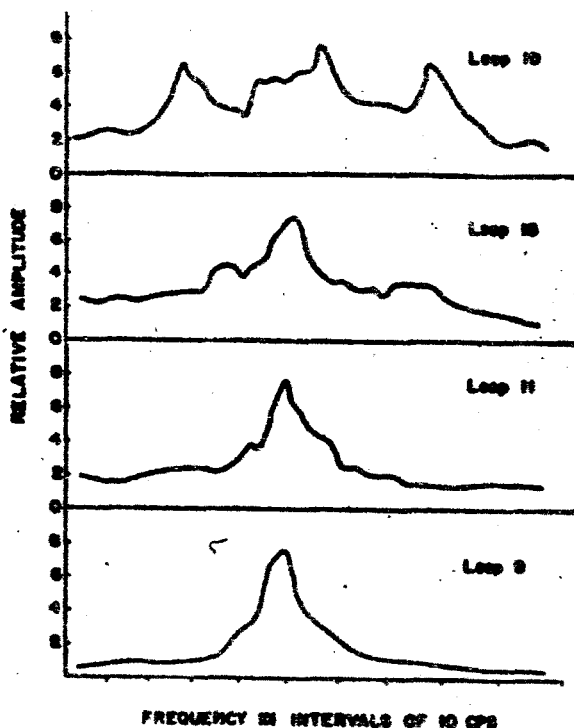


FIGURE 4.—Selected spectra obtained with the cross-correlating narrow-band filter. Corresponding sections of the chart-recording are labeled in figure 1.

ing for the noise power contained in the peaks of the spectra. The data so obtained are plotted in figure 2 for altitudes above 67 km. It can be seen that there is considerable scatter in the data.

It will be noted that the cross-correlating, narrow-band filter extended the receiver output measurements to 167 km altitude and to a level 25 db below that possible using the chart recordings. The sensitivity improvement that might have been expected is 24 db. This is based on an 18 db gain from a reduction in the predetection bandwidth from 50 to 0.85 cps, a 3 db gain from reduction of average noise power by the cross-correlation technique for an estimated duty cycle of 50% for NSS traffic, a 5 db gain from the post-detection averaging of each 4-second sample, and an estimated 2 db loss because of detector SNE reduction. This agreement between the observed and predicted performance of the correlating filter is surprisingly good.

The receiver output was referred to the receiver input through the receiver gain characteristic which was approximately logarithmic. For the data below 67 km, the receiver gain was set by NSS signal amplitude. For the data above 67 km, the receiver gain was set primarily by the noise in the receiver passband. The resulting curve of receiver input vs altitude is shown in figure 5. It can be noted that there is considerably less scatter in figure 5 than was present in the receiver output curve as shown in figure 2. This fact is the principal justification for the interpretation of the spectra of figure 4 as described above.

### MEASURED TOTAL ATTENUATION

In order to determine the variation of electric field strength with altitude, it was necessary to consider the antenna orientation and changes in the terminal impedance of the antenna. The antenna elements made an angle with the vertical of 70° and greater after the rocket entered the D-region. On the assumption that the wave normal in the whistler mode was vertical, the correction for antenna orientation was no more than 1 db and can be considered negligible. Measurements of the magnitude of antenna impedance during launch showed no significant variations until the shroud was jettisoned, although the impedance was different from that in free space because of the proximity of the third-stage rocket, solar paddles and epoxy shroud. The lack of significant variation in antenna terminal impedance before shroud ejection is believed to be due to the fact that the epoxy shroud shielded the antenna elements from electron and ion currents from the ionosphere.<sup>2</sup> With the effects of both antenna orientation and the change in antenna impedance being negligible, the curve of receiver input can be considered to represent the variation of relative electric field strength between about 50 and 162 km altitude.

Absorption calculations, described later, indicate that absorption begins about 10 km below the inflection point of the field strength curve, or about 60 km in this case. Assuming that the whistler-mode signal is launched into the ionosphere at this height, the measured

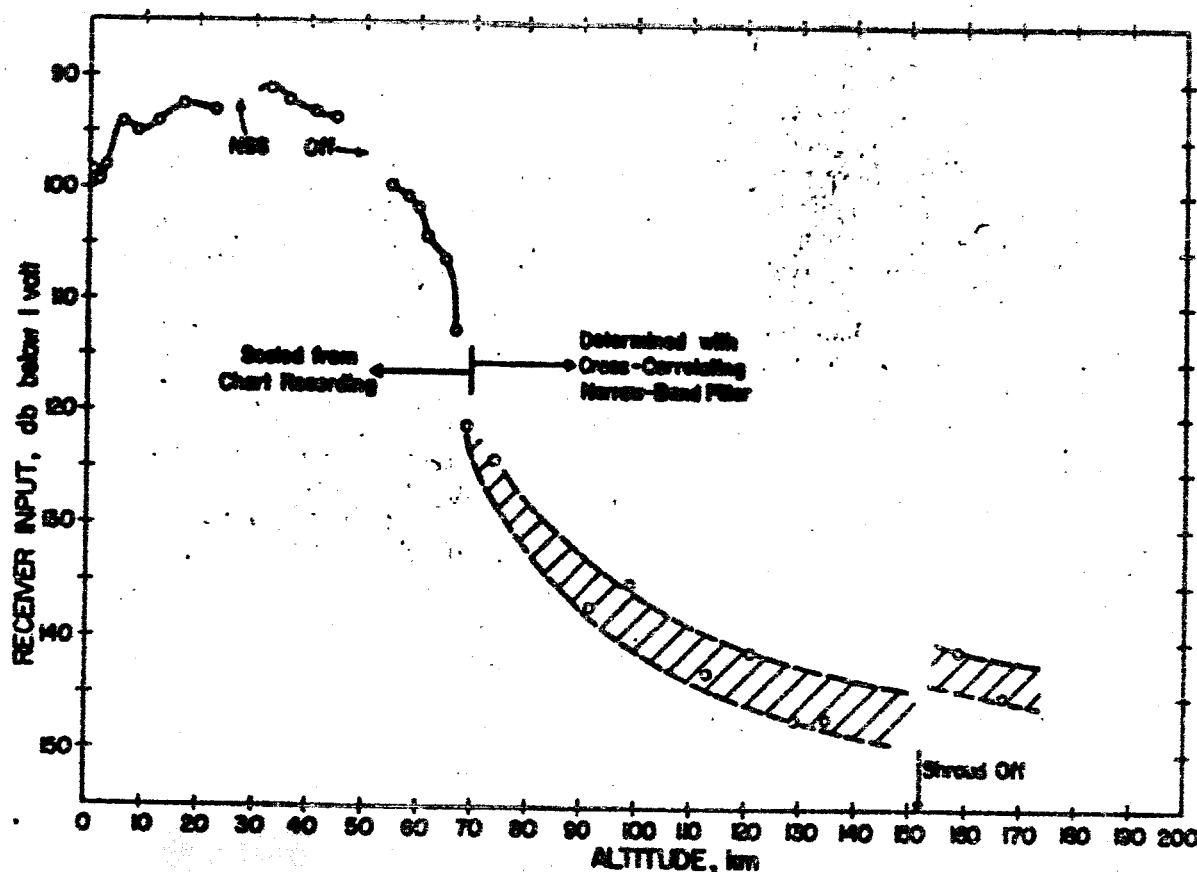


FIGURE 5.—Satellite receiver input level below 1 volt plotted vs. altitude. Data between about 60 and 158 km may be interpreted as relative variation of electric field strength within the ionosphere.

total attenuation through the lower ionosphere up to about 150 km is  $43 \text{ db} \pm 4 \text{ db}$  for daytime.

At heights below 60 km, the observed variation in signal strength appears to be explained by the waveguide-mode theory of VLF propagation.<sup>4</sup> Recent calculations of the height-gain effect by Wait and Spies<sup>5</sup> show that as altitude increases the intensity first increases, reaches a maximum, and then decreases to some fraction of the ground intensity at the ionosphere boundary. For parameters appropriate to this situation, these calculations do not show as great an increase in intensity for the low altitudes as the measurements show, and it must be taken into account that the distance to NSS decreased and that the relative amount of seawater path increased as the rocket ascended.

Whatever the influence of the last-mentioned factors, the variation near the ionosphere is predominantly due to the height-gain effect since there is little change in the path or distance for this altitude increment. And a priori choice of 70 km for an effective height of the lower edge of the ionosphere would be in agreement with that adopted by most workers who assume a homogeneous sharply-bounded ionosphere model for VLF calculations. The height-gain calculations<sup>6</sup> for an assumed ionosphere height of 70 km show a 6 db loss between 60 and 70 km. However, the measured loss between 60 and 70 km, as shown in figure 5, is about 17 db. This significant discrepancy further suggests that the effective height of the ionosphere and the beginning of absorption was more nearly 60 km at the time the measurements reported here were made.

## PREDICTED TOTAL ATTENUATION

Some preliminary calculations of whistler-mode absorption have been made at Stanford for various electron-density and collision-frequency models of the lowest ionosphere.<sup>6</sup> The daytime models are applicable to this experiment since the launch took place at about 0930 EST and the trajectory carried the satellite into longitudes of even later local time. The calculations show that almost all of the D- and E-region absorption occurs below about 130 km. Hence, the calculations can be considered to predict all the absorption up to 150 km. The first calculation utilized the electron-density profile deduced by Nertney<sup>7</sup> and the collision-frequency profile deduced by Nicolet,<sup>8</sup> and yielded a total absorption of 17 db. A second calculation utilized profiles of electron density and collision frequency which can be considered composite models deduced from the data given in the survey of Waynick,<sup>9</sup> and yielded a total absorption of 23 db.

Before the calculations can be compared with the measurements, there are several other sources of attenuation that must be considered. These include reflection losses and the effects of antenna polarization and changing wave impedance within the ionosphere. The loss due to reflection at the lower boundary of the ionosphere will be accounted for by considering only the direct ray. The higher-order reflected rays should be considerably attenuated by reflection from a daytime ionosphere. In this case, the subrocket point at the boundary of the lower ionosphere is just below the horizon. However, a consideration of diffractive effects in low frequency propagation by Wait<sup>10</sup> shows that the "cut-back factor" for this case is negligible. A computation of the transmission coefficient based on the work of Budden<sup>11</sup> shows that for the ordinary ray (whistler-mode) a reflection loss of 19 db occurs for a sharply-bounded, summer-daytime ionosphere model ( $u/\omega r = 0.6$ ,  $r = 60^\circ$ ). The extraordinary ray which is transmitted into the ionosphere is completely absorbed well below 150 km.

The change in wave impedance in the ionosphere results in attenuation since, for a given power density, the electric field strength varies

directly with the square-root of the wave impedance, and the wave impedance in the ionosphere is less than that of free space. This attenuation, assuming longitudinal propagation, is found to be 11 db between the lower boundary of the ionosphere ( $u/\omega r = 0.6$ ,  $r = 60^\circ$ ) and 150 km where the electron gyro-frequency and plasma frequency are estimated to be about 1.2 and 3.0 Mcps, respectively.

Just below the ionosphere, the incident electric field, consisting primarily of the direct ray, can be assumed to be vertical, while just within the ionosphere the field can be assumed to be circularly polarized in the horizontal plane.<sup>12</sup> Thus the antenna made an angle of  $70^\circ$  with the electric field just below the ionosphere, while making an angle of  $20^\circ$  or less with the horizontal field within the ionosphere. Polarization corrections based on these relative orientations amount to a gain of about 9 db. In addition, a loss of about 3 db is incurred because of the spatial averaging of the approximately circularly polarized whistler-mode component within the ionosphere by the linear satellite antenna.

Adding the above factors to the absorption gives the following tabulation for the estimated total attenuation through the summer-daytime ionosphere up to 150 km altitude:

Day Model	Total Absorption	Total Attenuation
Nicolet and Nertney.....	17 db	31 db
Composite.....	23 db	47 db

## DISCUSSION

It should be noted that the predictions outlined in the previous section were prepared assuming whistler-mode propagation along the magnetic field (assumed to be vertical here) for a constant incident electric field intensity at the lower ionosphere. The propagation path from Station NSS to the satellite did not quite provide constant field intensity in the ionosphere below the satellite. The course of the launch trajectory was in a north-easterly direction from Cape Canaveral and the average distance from Station NSS to the sub-satellite point for the altitude increment of 60 to 150 km was about 1,000 km and changed about 15%. Calculation for a comparable situation suggests



that the field strength just within the ionosphere would probably vary by about 3 db over this distance change.<sup>12</sup> This will be considered negligible here, and the predictions as given can be considered to apply to the measurements.

It can be seen that the total attenuation measurement of  $43 \text{ db} \pm 4 \text{ db}$  compares quite well with the calculated total attenuations of 41 and 47 db. The discrepancy is within the experimental errors and the magnitudes of the various effects which have been neglected in this analysis. It should be obvious that the calculations are only approximate since several 1 to 3 db effects have been neglected. However, the measurements also were only approximate since a rough estimate was used to select the altitude at which absorption began. Nonetheless, it appears that no unusual attenuation phenomena were observed and that the measured total attenuation can be accounted for by the analysis presented above.

Since the measurements which are reported here were made, the results of two relevant experiments have been reported. In the first experiment, the variation of Station NBA located at Summit, Panama Canal Zone (18.0 kc) signal strength with altitude up to about 115 km was measured at about 1700 local time on 14 March 1961 using a split-rocket electric dipole antenna.<sup>14</sup> Aspect data was not available for these measurements. Allowing for uncertainties in antenna orientation and such factors as diurnal and seasonal effects, these rocket measurements are quite consistent with those reported here.

The second relevant measurements were those made in the LOFTI I Satellite experiment.<sup>14, 15</sup> The total attenuation deduced from the LOFTI I measurements is somewhat different in that the detailed variation of signal strength with altitude was not obtained, although much more data on total attenuation was, of course, obtained. The measurements reported (ratio of apparent electric field intensity at the satellite to computed field intensity on the ground)<sup>14</sup> are also consistent with the measurements reported here when proper allowances are made for different measurement frequencies, the attenuation through the F-region and the different geometric factors for each case.

In conclusion, it appears that the launching of the whistler mode, at least in daytime, can be described to a first order by utilizing a sharply-bounded model of the ionosphere to account for the reflection-transmission phenomenon, and a slowly-varying model to account for the absorption experienced by the transmitted wave.

## REFERENCES

1. Space Technology Laboratories, Project Able-3 Final Mission Report Volume 2, August 1960.
2. Eorden, L. H., and Wolfram, R. T., VLF Instrumentation for the Able-3 and Able-4 Satellite Programs, SRI Final Report Proj. 2765, Stanford Res. Inst., February 1961.
3. Miodnosky, R. F., and Garriott, O. K., The v.l.f. Admittance of a Dipole in the Lower Ionosphere, Proc. Internat. Conf. on the Ionosphere, London, July 1962, pp. 484-491, The Institute of Physics and the Physical Soc., 1963.
4. Budden, K. G., The Waveguide Mode Theory of Wave Propagation, Prentice-Hall, New York, 1962.
5. Wait, J. R., and Spies, K. P., Height-Gain for VLF Radio Waves, J. Res. NBS, Vol. 67D, No. 3, pp. 183-188, March-April 1963.
6. Shih, K. K., Unpublished work.
7. Nertney, R. J., The Lower E and E Region of the Ionosphere as Deduced from Long Radio Wave Measurements, J. Atmos. Terr. Phys., Vol. 3, No. 2, pp. 92-107, 1953.
8. Nicolet, M., Collision Frequency of Electrons in the Terrestrial Atmosphere, Phys. of Fluids, Vol. 2, No. 2, pp. 95-99, March-April 1959.
9. Waynick, A. H., The Present State of Knowledge Concerning the Lower Ionosphere, Proc. IRE, Vol. 45, No. 6, June 1957.
10. Wait, J. R., Diffractive Corrections to the Geometrical Optics of Low Frequency Propagation, NBS Rept. 5572, U.S. Dept. of Comm., Natl. Bureau Stds., June 1958.
11. Budden, K. G., Radio Waves in the Ionosphere, Cambridge University Press, 1961.
12. Storey, L. R. O., An Investigation of Whistling Atmospherics, Phil. Trans. Roy. Soc. A, Vol. 245, pp. 113-141, 1953.
13. Bell, T. F., Halliwell, R. A., Miodnosky, R. F., and Smith, R. L., Geocyclotron Feasibility Study Radioscience Lab., Stanford Univ., Final Rept. Contract AF39(601)-4506, Chap. III, pp. 97-114, Jan. 1963.
14. Lomax, J. B., Measurement of VLF-Transmission Characteristics of the Ionosphere with Instrumented Nike-Cajun Rockets, Stanford Res. Inst. Final Rept. Contract N0w 40-0435(FBM), June 1961.
15. Lefphart, J. P., Zook, R. W., Beards, L. B., and

Toth, E., Penetration of the Ionosphere by Very-Low-Frequency-Radio Signals—Interim Results of the LOFTI I Experiment, Proc. IRE, Vol. 50, No. 1, pp. 6-17, Jan. 1962.

16. Rorden, L. H., Helliwell, R. A., and Smith, R. L., An Interpretation of LOFTI-I VLF Observations, Presented at AGARD Meeting, Munich, Germany 17-21 September 1962.